DATA-DRIVEN INVESTIGATION OF LATENT HEAT THERMAL ENERGY STORAGE PERFORMANCE UNDER DYNAMIC OPERATING CONDITIONS

Raman Safaee[1*], Phil Ward[2], Yulong Ding[3], Adriano Sciacovelli[3*]

[1] University of Birmingham, School of Chemical Engineering, Birmingham Centre for Energy Storage, Birmingham, United Kingdom

[2] Eskimo Products Ltd, Studio 53, Sydney Row, Spike Island, BS1 6UX, Bristol, United Kingdom

[1] University of Birmingham, School of Chemical Engineering, Birmingham Centre for Energy Storage, Birmingham Energy Institute, Birmingham, United Kingdom

*Corresponding Authors: r.safaee@bham.ac.uk
a.sciacovelli@bham.ac.uk

ABSTRACT

This paper presents a novel data-driven approach for characterizing the performance of Latent Heat Thermal Energy Storage (LHTES) systems employing Phase Change Materials (PCM) across a broad spectrum of operating conditions. LHTES systems are increasingly utilized in various sectors, notably in domestic space heating. Traditional research in this field has largely been confined to examining individual LHTES systems under fixed, predefined conditions. However, the practical deployment of these systems is expected to entail operation under a wide range of conditions, such as fluctuating heat transfer fluid (HTF) input temperatures, flow rates, and states of charge (SoC).

The study introduces and tests a comprehensive data-driven framework to characterize, under the wider possible spectrum of conditions, an LHTES prototype device (~1kWh, Ts ~ 42 – 43 °C) designed for building applications. Unique to the approach is its reliance on exclusively experimental data, which has been gathered through a comprehensive testing campaign. The proposed data-drive framework is employed to assess efficiency, heat transfer, inlet/outlet temperatures, and SoC, relying solely on experimental data. The findings of the study can provide sufficient inputs for data reduction techniques such as Respond Surface Methodology (RSM) and circumvent the need for high-fidelity parameters required in traditional first principle LHTES modeling.

The findings indicate that LHTES units maintain highly stable performance variations over different operating conditions. Notably, increasing the input temperature from 48 °C to 54 °C in charging operation reduces the full charging time by up to 100%, while variations in flow rate influence the performance by 5 to 50% depending on the Reynolds numbers and flow regimes. The HTF flow rate influence on the performance drastically decreases at Reynolds numbers around 6500, which corresponds to turbulent flow regime characterized with high internal heat transfer coefficient. Overall, this research addresses the critical need for in-operando characterization of LHTES systems, leveraging the increasing availability of real-time data. The limited prior research in this specific area underscores the novelty and importance of the work, marking an advancement in the understanding and application of LHTES technologies.

1 INTRODUCTION

Thermal Energy Storage (TES) technology is considered an attractive topic in energy storage due to its simplicity and high energy density potential. TES technologies are categorized in three main categories named sensible heat storage, latent heat storage, and thermo-chemical heat storage (Gao et al. 2023). Among the TES technologies, Latent Heat Thermal Energy Storage (LHTES) is considered one of the most interesting ones which has gathered considerable attention in recent decades and plenty of studies have been carried out on the design and performance level either on the material or the energy system

https://doi.org/10.52202/077185-0098

scale. The present study is dedicated to evaluating the performance of LHTES units tailored for low-temperature domestic space heating applications. The evaluation takes place by a systematic experimental approach that assesses unit performance under dynamic operating conditions and provides useful insights on device in-situ performance in real-life application.

Research on TES application in the space heating sector is abundant in the literature. The TES integration in heating/cooling systems are covered for a variety of systems at broad temperature ranges. The application includes sensible heat energy storage (He et al. 2022; Kuznik et al. 2020), latent heat energy storage (Hassan et al. 2022) and thermochemical energy storage (Kant and Pitchumani 2022).

Moreover, the application of TES in conjunction with carbon-free heating technologies including electric heaters and heat pumps have been extensively studied as attractive topics in this area. A study by Kou and Wang (Kou and Wang 2023) thermodynamically evaluates the application of TES devices integrated to electric heaters and heat pumps and provides valuable insights on energy conversion and exergy efficiency. Another study by Lu et al. works on design optimization of a latent heat thermal energy storage device for peak load-shaving scenarios for an office building (Lu et al. 2022). Research on integrating TES to solar thermal systems are also interesting and well-addressed in the literature, one is discussed by Yildiz et al. which experimentally explores the performance of a solar-assisted heat pump integrated to a TES unit (Yıldız et al. 2023).

Experimental studies and data-driven approaches is found to be abundant in the literature for LHTES systems. The research studies cover experimental data on a wide range from encapsulated PCM heat exchangers(Y. Zhang et al. 2024) to finned tube heat exchangers (Herbinger and Groulx 2022; X. Y. Zhang et al. 2024) which is the case in the present study. The performance of PCM-integrated finned tube heat exchangers over a wide range of input conditions, however, is not well addressed in the literature, which is the point this study is dedicated to shed light on. The operating conditions in this study are chosen based on heat pump operating constraints, due to the attractivity of heat pump integrated TES system applications in space heating sector. In another interesting study, Saydam et al. experimentally studied the performance of a helical coil heat exchanger submerged in Paraffin wax as PCM, which proved that the effect of charging temperature is more significant than the flow rate. It has also been pointed out that the flow rate change does not seem to influence the discharge phase (Saydam et al. 2019). In another study (Herbinger and Groulx 2022), a finned tube heat exchanger submerged in PCM (Dodecanoic acid) is analyzed for pressure drop and heat transfer characteristics. The impact of geometry, configuration, and operational parameters are discussed, and it is pointed out that the temperature differential between the HTF and the PCM is crucial in determining the heat transfer rate in the system.

In light of the discussed arguments in the literature, it is noted that experimental and thermodynamic studies on LHTES systems in the literature are abundant and cover a wide range of systems; however, a systematic approach over fully dynamic operating conditions for LHTES technology seems rare. And the present study can enlighten LHTES unit response to a variety of operating conditions and provide inputs for system in-situ performance predictions.

2 SCOPE AND OBJECTIVES

The overarching objective of the present paper is experimental performance characterization of a latent heat thermal energy storage device designed and tailored for low-temperature space heating applications in buildings. The experimental campaign is performed on a 1-kWh LHTES test piece, tested under several combinations of operating conditions to provide insights on device in-situ performance in real applications. The dynamic characteristic of the experiments is achieved through imposing a unique operating condition (temperature, HTF flow rate) combination at each experiment case.

This study and produced results will have relevance for a variety of TES-integrated heating technologies including electric heaters and heat pump systems. The operating range chosen for experiments have been tailored to cope with all heating technologies including boilers and heat pumps (Chesser et al. 2021).

The data-driven approach adopted in the present study focuses on the effect of charging temperature and flow rate on the charge/discharge behavior of LHTES devices. The device performance over the

https://doi.org/10.52202/077185-0098

operating condition range is assessed through a selection of performance indicators including heat transfer rate, charging/discharging time, and State-of-Charge trends.

3 SYSTEM DESCRIPTION

In order to be able to effectively evaluate the performance of LHTES units using experimental approaches, a competent test rig is required to emulate variable operating conditions present in the built environment. The final installation site envisioned for the present LHTES device is a fully electric or heat pump driven system due to low emissions and high energy efficiency. A schematic showing the final configuration of the LHTES device in the built environment is depicted in **Figure *1***. The test set-up required for device testing, is designed and realized in a way to effectively emulate the situation occurring in the final built environment illustrated in **Figure *1***.

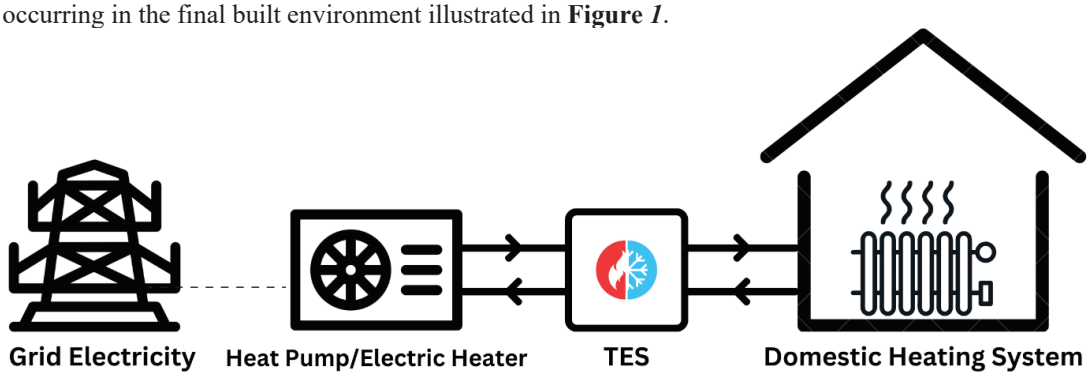

Figure 1: LHTES device application in the built environment

The realized test rig provides hot water at a constant temperature to emulate the hot water production by a heat pump or electric heater. The water temperature is limited to the limits of domestic heat pump heat generation (Chesser et al. 2021). The heat discharge by domestic heat distribution technologies (radiators, underfloor heating, etc.) is also emulated using an air-cooled heat exchanger which follows the same working principle. Using the mentioned system principles, the operating conditions including flow temperature and flow rate are altered and the device performance is observed at each case.

4 METHODOLOGY

The experimental campaign in the present study is carried out on a 1-kWh Latent Heat Thermal Energy Storage (LHTES) prototype consisting of a finned tube heat exchanger (copper tube and aluminum fins) placed intercalated with selected Phase Change Material (PCM) and confined in an aluminum casing. The selected PCM is an organic PCM named OM42 manufactured by PLUSS Advanced Technologies. The thermo-physical properties of the selected PCM are provided in Table 1.

The operating conditions – chiefly operational temperature range – within scope of this work have been selected to have relevance with the general trend of zero-carbon heating in buildings. Specifically, maximum and minimum temperature considered during the experimental testing of the LHTES system have been chosen to be compatible with domestic heating generated by heat pumps and delivered by low-temperature heating systems, such as underfloor heating systems. In this sense the process for the Phase Change Material (PCM) was meticulously conducted, taking into consideration the typical heat pump's supply temperature as well as the minimum temperature requirements of domestic heating systems. Specifically, literature indicate heat pumps maximum supply temperature to be about 55 °C, which would correspond to the lowest acceptable COP - coefficient of performance (Chesser et al. 2021; Famiglietti et al. 2023). Conversely, literature suggests that 40 °C is a typical operating temperature for modern low-temperature heating systems such as underfloor heating (Yang et al. 2022). Therefore, commercial PCM (PLUSS OM42 – melting temperature of 42°C) was considered as it aligns with the operational temperature of the heat pump during charging but also meets the critical temperature thresholds necessary for LHTES discharging and domestic heating delivery. Thus, by adhering to these

https://doi.org/10.52202/077185-0098

criteria, the selection implies experimental testing at conditions relevant for energy efficiency within residential heating applications (Chesser et al. 2021; Famiglietti et al. 2023; Yang et al. 2022).

Table 1: PLUSS OM42 thermophysical properties

Property	Value	Unit
Phase transition temperature	42 – 44	°C
Latent heat	195	kJ/kg
Average specific heat	2.75	kJ/kgK
Average density	880	Kg/m^3
Average thermal conductivity	0.15	W/mK

4.1 Experimental set-up

The experiments on the mentioned TES heat exchanger are carried out using a test rig designed and assembled in University of Birmingham for TES performance testing. The test rig emulates domestic heating environment for the TES device and it is composed of a closed-loop water recirculation circuit with a hot water tank, a 3-kW immersion electric heater, an air-cooled heat exchanger, circulator pumps, manual and motorized valves, and measuring devices such as thermocouples, thermistors, pressure transducers and flow meters. A schematic and photo of the realized test rig is provided in Figure 2.

The experiment execution protocol is to insert a set temperature for the circulating water, having the water recirculation until the set temperature is reached (excluding the TES at this step), including the TES device and start charging, exclude the water tank at the end of the charging period and including the air-cooled (cooling) heat exchanger (discharge period). At the end of the discharge period, the system is set back to the initial setting to prepare for the next round of experiments. The principles at which the test rig is operated is to emulate the charge and discharge operation of a TES device in the domestic heating environment described in the system description section.

The immersion heater and circulating pumps are controlled by PID controllers, which ensures prompt control over the required variables. The air-cooled (cooling) heat exchanger is rated at 3kW and releases the heat stored in the TES to the surrounding environment. The actual average discharged power is observed to be about 2 kW due to lower ΔT than the rated design conditions.

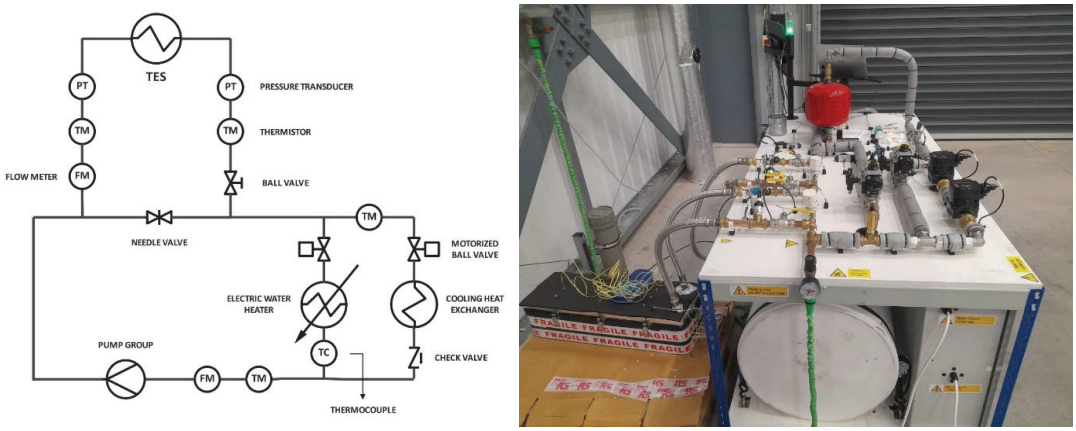

Figure 2: Experimental set-up configuration

4.2 Design of experiments

The experiments performed on the TES unit, as discussed previously, are tailored to emulate the operation in a typical domestic heating environment. Therefore, certain limitations are respected to effectively assess device performance in the built environment. The charging temperature is set between 48 °C and 54 °C to respect maximum supply temperature by a variety of heat pumps. The minimum charging temperature is set based on practical experience on TES charging which suggests a minimum 6 – 8 °C temperature gap between the charging temperature and PCM melting point to ensure full phase transition. The flow rates are analyzed in the range 5 – 15 l/min which are found to be an average flow

https://doi.org/10.52202/077185-0098

rate for domestic-scale heat pumps. The actual input parameters in each experiment case are provided in
Table ***2***.

Table 2: Design of Experiments

	Case 1	Case 2	Case 3	Case 4	Case 5	Case 6	Case 7	Case 8
Charging temperature	48 °C	48 °C	48 °C	50 °C	50 °C	50 °C	52 °C	54 °C
Flow rate	10 l/min	15 l/min	5 l/min	10 l/min	15 l/min	5 l/min	10 l/min	10 l/min
Discharge rated power	3 kW	3 kW	3 kW	3 kW	3 kW	3 kW	3 kW	3 kW

The above-mentioned set of experiments will allow us to experimentally assess the impact of HTF flow rate and input temperature on the device performance and provide insights on favorable conditions for optimized operation of the TES device.

4.3 Data collection and processing procedure

The required data in the present analysis is provided by experimental data collected by two separate dataloggers on the test rig side and prototype side.. The test rig datasets contain data related to the test rig parameters including flow rates, pressure and temperature of various points within the test rig circuit including the flow inlet and outlet of the TES heat exchanger. The flow rates are measured using an Omega FTB series turbine flow meter and an RS radial flow meter. The pressures and temperatures are measured through Sick PBT series pressure sensors and ATC Semitec pipe clip temperature sensors (thermistors) respectively. On the Prototype (PCM) side, the temperature data in real time is recorded on a separate Picolog TC-08 datalogger, which allows us to record PCM temperature data using type K thermocouples in real time. The inserted thermocouples in the PCM tank are placed in depths of 6mm and 12 mm for the measurements to account for different locations within the heat exchanger. The positioning of the thermocouples within the PC tank is illustrated in Figure 3. All the recorded data including the PCM, and the test rig data are collected at 1 Hz frequency.

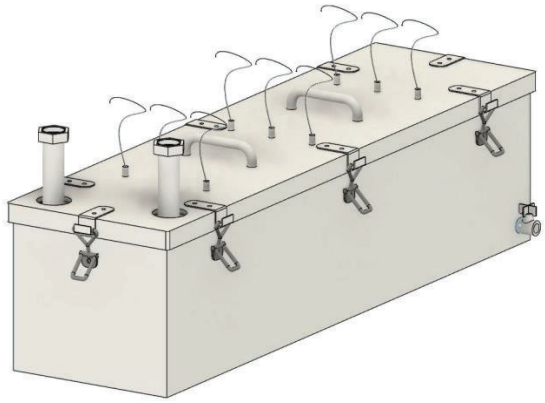

Figure 3: LHTES Prototype CAD model

4.4 Key performance indicators and data analysis

In order to analyze the experiment results in a systematic way and to be able to critically review and assess the produced datasets, some parameters marked as performance indicators are selected and highlighted throughout this document. The chosen parameters allow us to draw conclusions based on extracted evidence on visual results. The main parameters chosen in this study are the PCM temperature variations, the HTF input and output temperatures, the heat transfer rate between the HTF and the PCM, the thermal conductance between the PCM and the HTF, and finally the sate-of -charge, all of which are analyzed in real time during charge and discharge operations.

https://doi.org/10.52202/077185-0098

The main performance indicators used in this analysis are briefly introduced and the relevant equations are discussed followingly.

4.4.1 PCM average temperature: The PCM temperature measurements of each specific thermocouple and their linear average value are used to estimate the charge/discharge time based on the temperature trend. The positioning of the thermocouples within the storage medium is done in a way to measure a uniformly spread distribution of points to produce accurate temperature results.

4.4.2 Heat transfer rate: An important performance indicator introduced in this paper is the heat transfer rate between HTF and the PCM, which is calculated using equation (1):

$$P = mC_p\Delta T \tag{1}$$

where P, m, C_p, and ΔT stand for the exchanged power (heat transfer rate) in kW, the HTF flow rate in kg/s, the HTF specific heat and temperature differential between the HTF inlet and outlet of the device. The calculation of heat transfer rate not only reveals insights about the required power to be supplied to the unit by the heat generator in real time, but also generates the required input for State-of-Charge estimation in the following sections.

4.4.3 Thermal conductance (resistance): the thermal conductance between HTF and the PCM, is calculated using the LMTD method to simulate the heat transfer phenomena within the heat exchanger. The thermal conductance (UA) in W/K is calculated using the heat transfer equation (2):

$$UA = \frac{q}{\Delta T_{lm}} \tag{2}$$

In the above equation, q, and ΔT_{lm} stand for the heat transfer rate and the Mean Logarithmic Temperature Difference respectively. The total thermal resistance is calculated as the reciprocal of the thermal conductance in equation (2).

4.4.4 State-of-Charge: The estimation of the State of Charge (SoC) of thermal energy storage units is of great importance in the in-site operation of units, as there is the need for the system to monitor the SoC and act accordingly in charge and discharge process. SoC estimation for thermal energy storage has been previously studied in the literature and several solutions have been proposed. A summary of the methods and solutions for state of charge monitoring is provided by Zsembinszki et al. (Zsembinszki et al. 2020), which lists the SoC evaluation methods into 4 methods based on average PCM temperature, average PCM specific enthalpy, energy balance on heat transfer fluid and the pressure inside the PCM cavity. The present paper explores the methods based on HTF energy balance and PCM enthalpy which are often the methods adopted in the literature.

SoC estimation based on HTF energy balance: Evaluation of thermal energy storage SoC based on an energy balance of the Heat Transfer Fluid (HTF) is one of the well-known methods used in several studies in the literature (Bastida, De la Cruz-Loredo, and Ugalde-Loo 2023; Beyne et al. 2022). This method estimates the SoC based on the energy being transferred to/from the TES unit during the charge/discharge process. An advantage of this method over the average PCM method is the higher accuracy of the SoC monitoring in both the latent and the sensible phase. However, this method does not take the device heat loss into account, and often there will be a discrepancy in the unit charged and discharged energy due to some of the heat being lost during the charging or storage period. Equation (3) provides the mathematical formula for SoC calculation based on HTF energy balance:

$$SoC\ [\%] = \frac{\int_0^{t_i} P.dt}{\int_0^{t_f} P.dt} \times 100 \tag{3}$$

In which P, t_i, and t_f are the exchanged power between the HTF and the TES, the time at step i, and the time step at the end of the process respectively.

SoC Estimation based on PCM enthalpy: The average PCM enthalpy method tracks the PCM temperature and translates the PCM temperature into enthalpy and defines the SoC equation based on PCM enthalpy. The advantage of such a method with respect to the average temperature method is that it can accurately track the actual state of charge trend due to using the enthalpy curve instead of the temperature curve. This method inherently reacts to unit heat loss and therefore does not experience the drawbacks of HTF energy balance method. The SoC calculation formula according to Zsembinszki et al. (Zsembinszki et al. 2020) is provided in equation (4):

$$SoC\ [\%] = \frac{h_i - h_{min}}{h_{max} - h_{min}} \times 100 \tag{4}$$

https://doi.org/10.52202/077185-0098

In the above equation, h_i, h_{min}, h_{max} are the enthalpy at time step i, the minimum and the maximum PCM enthalpy respectively.

Tracking the PCM enthalpy in two phase regions can be challenging due to very low temperature variations during phase transition. A widely studied simplified model to be able to accurately track PCM enthalpy during phase change is the so-called Apparent Heat Capacity Model, which has been extensively adopted in the literature for TES modeling(El Ouali et al. 2022) and state of charge estimations(Scharinger-Urschitz et al. 2020). The present paper simulates the apparent heat capacity of the PCM using a sigmoid function suggested by Yang and He (Yang and He 2010) and based on the DSC curve of OM42. The SoC value using such method is calculated using equation (5) as stated below:

$$SoC\ [\%] = \frac{\int_{T_1}^{T_i} C_{p,app} dT}{\int_{T_1}^{T_f} C_{p,app} dT} \times 100 \tag{5}$$

$C_{p,app}$ and subscripts 1, i, and f stand for the apparent heat capacity, reference time, time step i, and the final time step during the process respectively.

5 RESULTS AND DISCUSSION

The initial results of the experimental campaign are provided in Figure 4, Figure 5, and Figure 6, which show the different cases results at 48°C charging temperature, 50 °C charging temperature, and 10 LPM variable charging temperature respectively. For each experiment case, three performance figures representing the HTF input and output temperatures, the PCM temperature across the device enclosure, and the heat transfer rate over time are provided.

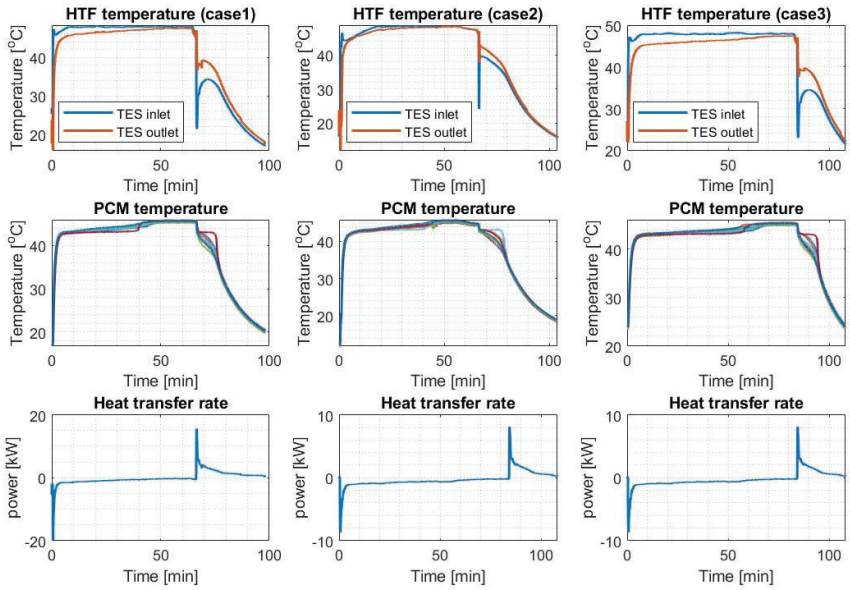

Figure 4: Performance curves, experiment cases 1, 2, and 3

An initial understanding over the provided results, is the maximum PCM temperature in the charging process which tends to keep a certain distance with the HTF charging temperature. In all cases it is observed that the PCM temperature will steady at a temperature 3 – 4 °C lower than the actual charging temperature. This can be due to a very low heat transfer rate in the final quarter of the charging period, and the inevitable heat loss of the unit, which at some point compensates for the small heat gain and causes the device to reach thermal equilibrium. Therefore, it is necessary to maintain a minimum 4 °C temperature gap between the charging temperature and the melting temperature to ensure full phase transition. The heat transfer data at the final quarter of the charging period reveals the unit heat loss, which is about 100 – 200 W depending on the device temperature.

https://doi.org/10.52202/077185-0098

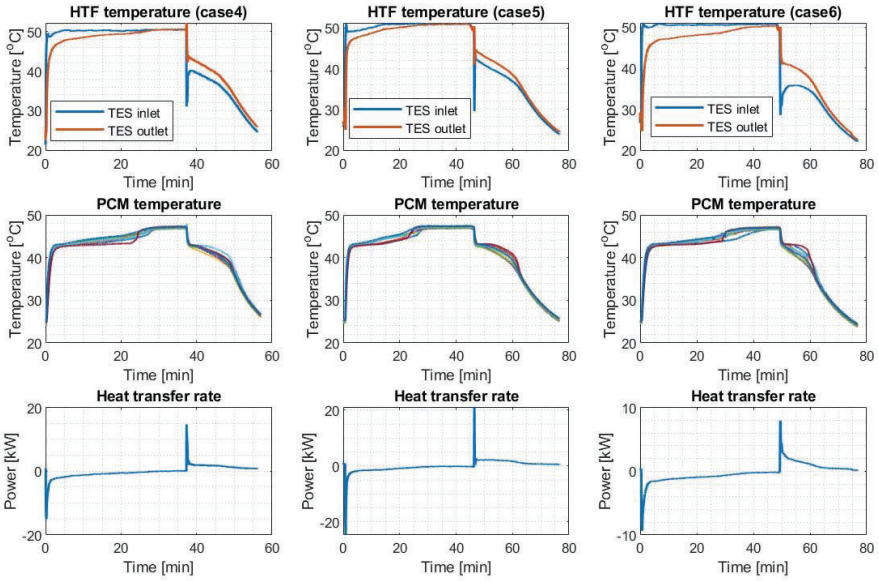

Figure 5: Performance curves, experiment cases 4, 5, and 6

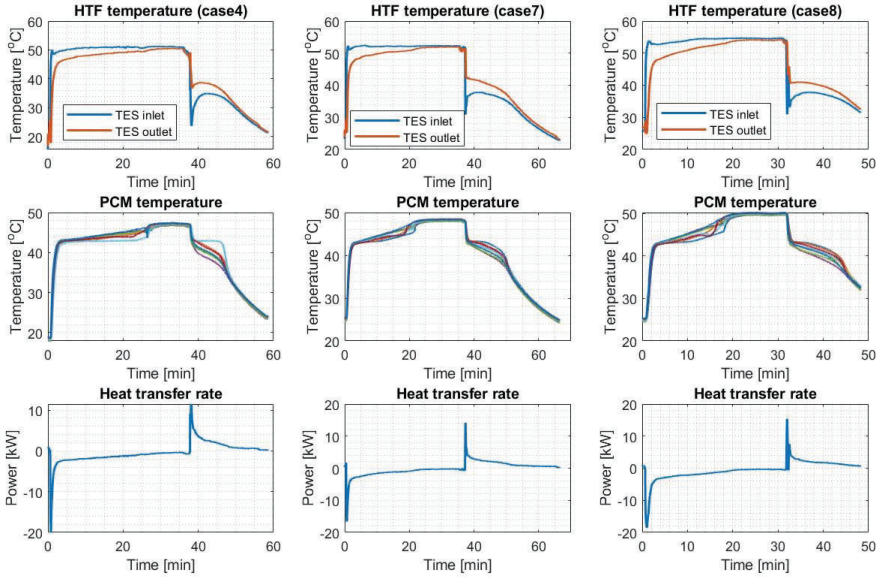

Figure 6: Performance curves, experiment cases 4, 7, 8

The heat transfer rate graphs in all cases display drastic spikes at the beginning of the charge and discharge process. Such a behavior which is common for LHTES systems and present in the similar works in the literature (Zauner et al. 2016; X. Y. Zhang et al. 2024), is primarily due to the large temperature difference between HTF and the heat exchanger enclosure at the beginning of the operation. The average heat transfer rate during the charging phase ranges from 700 up to 1900 W, depending on the HTF flow rate and the charging temperature. It is noticed that the flow rate impact on the average heat transfer rate is limited up to 10%, while the charging temperature seems to have a considerable effect on the average heat transfer rate causing an increment of 130% passing from 48 °C to 54 °C charging temperature.

https://doi.org/10.52202/077185-0098

Present analysis on the transferred energy in the charging period in all cases shows that between 40% and 60% of the total energy is transferred in the beginning quarter. An interesting observation is that the HTF flow rate has a direct impact on the heat transfer in the beginning period and therefore the cases characterized with higher flow rates are associated with the highest energy exchange in the beginning quarter of operation. This finding can provide useful insights on the power draw curve for electric or heat-pump-powered in-situ operations.

Following the PCM temperature curve in charge operations can deepen our understanding on the influence of temperature and HTF flow rate on the charging timespan. The average PCM temperature (linear average of all thermocouple measurements) is plotted in **Figure *7*** showing the PCM temperature trend in the charging period for a variety of charging temperatures (left-hand-side) and flow rates (right-hand-side). The left-hand-side figure approves the basic heat transfer principle which suggests that the heat transfer rate is linearly proportional to the temperature differential (ΔT) between the hot and cold media. The difference in the charging timespan, however, seems to be non-linear when approaching low temperatures., which is believed to be due to system heat losses during the charging operation which lessens the effective heat absorbed by the unit during charging operation. A separate analysis on the impact of flow rates on the performance of the LHTES prototype is performed and illustrated on the right-hand-side figure. A decrease in the charging time has been noticed moving from 5 LPM to 10 LPM which can be justified considering increasing Reynolds number and convective heat transfer coefficient within the tubes. However, very similar behavior has been observed between 10 and 15 LPM, which could undermine the accuracy of the experiments. Thus, to ascertain the testing accuracy, the device is tested at an intermediate flow rate equal to 7.5 LPM, and the results are reported together with other cases in the right-hand-side of **Figure *7***.

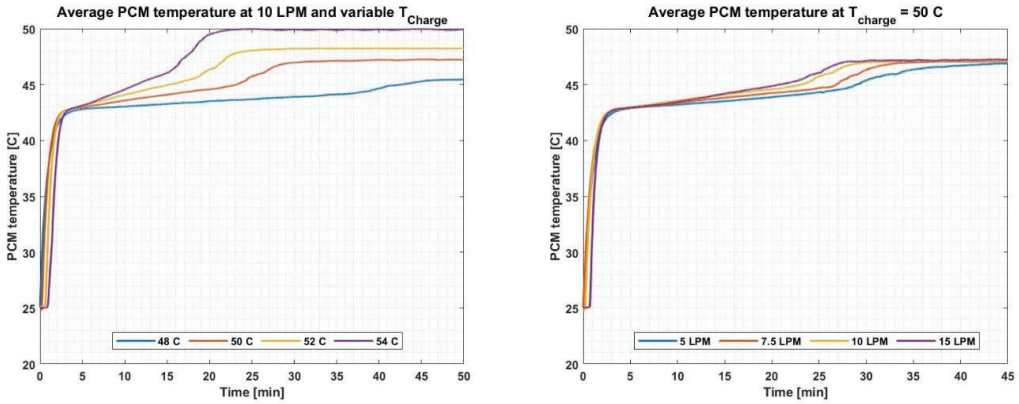

Figure 7: PCM average temperature over charging period

The new experiment results (carried out at 7.5 LPM) approve the previous experiments and highlight the fact that the flow rate has a considerable effect on the charging timespan but not on the final PCM temperature. It is observed that the charging time reduces by about 50% increasing the HTF flow rate from 5 to 10 LPM. But a similar increment on the flow rate from 10 to 15 LPM does not seem to have a significant effect on the device's performance. Such a behavior can be better understood by analyzing the heat conductance within the LHTES prototype.

The heat transfer phenomena within the device are driven by the heat conductance of the heat transfer fluid, tube wall, PCM and the fins (Tay et al. 2014), out of which the HTF side conductance is the variable in this analysis. Flow regimes in internal flow and the actual transition from laminar to turbulent flow has been extensively studied in the literature for a variety of geometries. The transition range for circular horizontal tubes which is the case in this study, has been claimed to be between 2000 and 4000 in many well-known correlations including Shah's and Churchill's (Ghajar and Madon 1992; Meyer and Olivier 2011). Corresponding Reynolds numbers provided in **Table *3*** show that
the lowest flow rate at 5 LPM, corresponds to transitional flow regime, which ultimately results in relatively low convective heat transfer coefficient on the HTF side. Whereas the 10 and 15 LPM cases are characterized with turbulent flow regime.

https://doi.org/10.52202/077185-0098

. The corresponding Reynolds number for each case is provided in **Table *3***.

Table 3: Reynolds numbers associated with tested flow rates

Flow rate	5 LPM	7.5 LPM	10 LPM	15 LPM
Reynolds Number	3250	4870	6500	9740

Considering the total heat conductance of the prototype in the charging period according to equation (2) (about 40 – 60 W/K) and the internal convection flow conductance at 15 LPM (about 4000 W/K), it can be deduced that within the fully turbulent region, the heat transfer coefficient of the internal flow is so high that the heat transfer phenomena is driven by the PCM-side only. The findings of this paper suggest that the corresponding Reynolds number to this phenomenon is about 6500 for the present LHTES prototype which is a horizontal finned tube heat exchanger.

6 STATE-OF-CHARGE ESTIMATION

The calculation logic over the estimation of the device state-of-charge (SoC) follows the definitions and equations presented in section 4.4, in which SoC estimation based on HTF energy balance and PCM enthalpy is discussed. SoC curves for a selection of cases using both methods are provided in **Figure *8***.

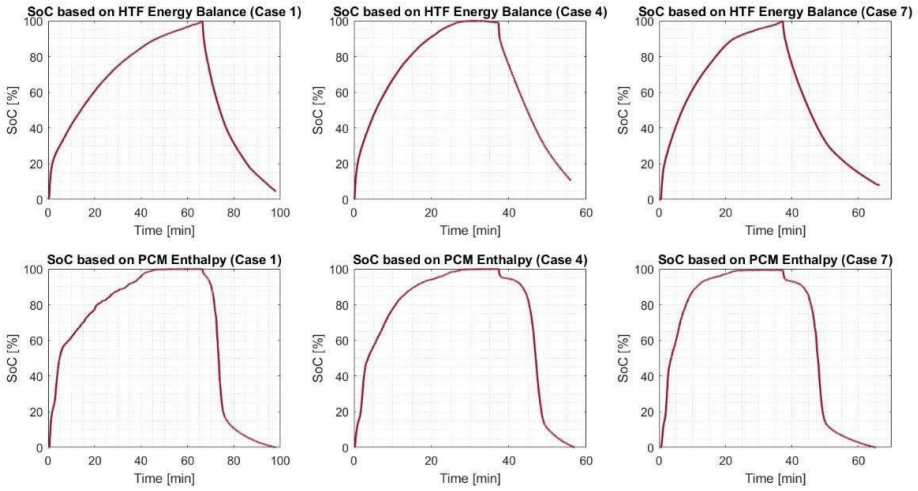

Figure 8: SoC trend based on HTF balance and PCM enthalpy

In light of the visual data presented in Figure 8, the SoC estimation based on HTF energy balance accurately reflects the SoC trend in both charge and discharge operations. The decreasing curve slope during charge/discharge is in agreement with the the heat transfer rate curve in this study and the literature. The draw-back of such analysis is the failure to capture the unit heat loss into account, which can result in high inaccuracy in the SoC estimation in cases with considerable unit storage time.. A common remedy adopted in the literature (Bastida et al. 2023), is to insert a PCM temperature monitoring element to the SoC calculation formula to rectify the heat loss discrepancy issue.

The PCM enthalpy method in calculating the SoC can be a more accurate one due to the SoC calculation based on real time PCM temperature, which perfectly captures any unit heat loss. However, the accuracy of the SoC tracking depends largely on the adopted enthalpy estimation method. Apparent heat capacity method (Yang and He 2010) can be a useful technique to relate PCM temperature to the enthalpy based on DSC curves and realistically track the SoC during operation.

7 CONCLUSIONS

In this paper, an experimental data analysis on a Latent Heat Thermal Energy Storage prototype is performed using a data-driven approach. Experimental data are extracted from a testing campaign on a

https://doi.org/10.52202/077185-0098

1-kWh finned tube heat exchanger under a variety of operating conditions. Experimental results on charge/discharge timespan, heat transfer rate, and state-of-charge are produced and discussed accordingly.

The findings of the paper suggest that the heat transfer rate experiences a drastic decline over the first few minutes and about 50% of the charge/discharge process occurs in the first quarter of the operations. The charging temperature considerably impacts the charging time and the average heat transfer rate during operations, so that the charging timespan shortens by more than 100% increasing the charging temperature from 48°C to 54°C. it is also noticed that the charging process elongates drastically approaching the PCM melting temperature. In the present set of experiments, it has been deemed unfeasible to charge the LHTES prototype by a charging temperature gap (between HTF inlet and PCM melting temperature) lower than 6 °C due to the presence of unit heat loss.

Findings on the impact of flow rates to the unit performance reveal that the HTF flow rate affects the charge/discharge behavior of the unit only if the internal flow regime within the unit is in the laminar/transitional region. It has been noticed that in case of a fully turbulent flow at Reynolds numbers above 6500 on the HTF side, the heat transfer phenomena will be driven by the PCM side, and the device performance is not expected to vary with flow rate variations.

An analysis on the SoC estimation based on HTF energy balance and PCM enthalpy balance, shows more accurate estimation of the SoC trend with the energy balance method, but failing to reflect the heat loss of the system during storage hours is a disadvantage of the method which can be addressed by adding an active PCM temperature element into calculations. The present study can be complimented by future experimental analyses on variable charge/discharge power and discharge temperature, which can lead to interesting statistical analyses including Response Surface methodology to capture the device performance under a wide range of operating conditions.

REFERENCES

Bastida, Hector, Ivan De la Cruz-Loredo, and Carlos E. Ugalde-Loo. 2023. "Effective Estimation of the State-of-Charge of Latent Heat Thermal Energy Storage for Heating and Cooling Systems Using Non-Linear State Observers." *Applied Energy* 331. doi: 10.1016/j.apenergy.2022.120448.

Beyne, Wim, Kenny Couvreur, Ilya T'Jollyn, Steven Lecompte, and Michel De Paepe. 2022. "Estimating the State of Charge in a Latent Thermal Energy Storage Heat Exchanger Based on Inlet/Outlet and Surface Measurements." *Applied Thermal Engineering* 201. doi: 10.1016/j.applthermaleng.2021.117806.

Chesser, Michael, Pádraig Lyons, Padraic O'Reilly, and Paula Carroll. 2021. "Air Source Heat Pump In-Situ Performance." *Energy and Buildings* 251. doi: 10.1016/j.enbuild.2021.111365.

Famiglietti, Jacopo, Tommaso Toppi, Davide Bonalumi, and Mario Motta. 2023. "Heat Pumps for Space Heating and Domestic Hot Water Production in Residential Buildings, an Environmental Comparison in a Present and Future Scenario." *Energy Conversion and Management* 276. doi: 10.1016/j.enconman.2022.116527.

Gao, Xinyu, Zhaoyang Niu, Xinyu Huang, Xiaohu Yang, and Jinyue Yan. 2023. "Thermo-Economic Assessments on Building Heating by a Thermal Energy Storage System with Metal Foam." *Case Studies in Thermal Engineering* 49. doi: 10.1016/j.csite.2023.103307.

Ghajar, Afshin J., and Khushrow F. Madon. 1992. *Pressure Drop Measurements in the Transition Region for a Circular Tube with Three Different Inlet Configurations*.

Hassan, Faisal, Furqan Jamil, Abid Hussain, Hafiz Muhammad Ali, Muhammad Mansoor Janjua, Shahab Khushnood, Muhammad Farhan, Khurram Altaf, Zafar Said, and Changhe Li. 2022. "Recent Advancements in Latent Heat Phase Change Materials and Their Applications for Thermal Energy Storage and Buildings: A State of the Art Review." *Sustainable Energy Technologies and Assessments* 49. doi: 10.1016/j.seta.2021.101646.

He, Zhaoyu, Abdul Samad Farooq, Weimin Guo, and Peng Zhang. 2022. "Optimization of the Solar Space Heating System with Thermal Energy Storage Using Data-Driven Approach." *Renewable Energy* 190:764–76. doi: 10.1016/j.renene.2022.03.088.

Herbinger, Florent, and Dominic Groulx. 2022. "Experimental Comparative Analysis of Finned-Tube PCM-Heat Exchangers' Performance." *Applied Thermal Engineering* 211. doi: 10.1016/j.applthermaleng.2022.118532.

 https://doi.org/10.52202/077185-0098

Kant, K., and R. Pitchumani. 2022. “Advances and Opportunities in Thermochemical Heat Storage Systems for Buildings Applications.” *Applied Energy* 321.

Kou, Xiaoxue, and Ruzhu Wang. 2023. “Thermodynamic Analysis of Electric to Thermal Heating Pathways Coupled with Thermal Energy Storage.” *Energy* 284. doi: 10.1016/j.energy.2023.129292.

Kuznik, Frédéric, Oliver Opel, Thomas Osterland, and Wolfgang K. L. Ruck. 2020. “Thermal Energy Storage for Space Heating and Domestic Hot Water in Individual Residential Buildings.” Pp. 567–94 in *Advances in Thermal Energy Storage Systems: Methods and Applications*. Elsevier.

Lu, Shilei, Quanyi Lin, Yi Liu, Lu Yue, and Ran Wang. 2022. “Study on Thermal Performance Improvement Technology of Latent Heat Thermal Energy Storage for Building Heating.” *Applied Energy* 323. doi: 10.1016/j.apenergy.2022.119594.

Meyer, J. P., and J. A. Olivier. 2011. “Transitional Flow inside Enhanced Tubes for Fully Developed and Developing Flow with Different Types of Inlet Disturbances: Part I - Adiabatic Pressure Drops.” *International Journal of Heat and Mass Transfer* 54(7–8):1587–97. doi: 10.1016/j.ijheatmasstransfer.2010.11.027.

El Ouali, A., Y. Khattari, B. Lamrani, T. El Rhafiki, Y. Zeraouli, and T. Kousksou. 2022. “Apparent Heat Capacity Method to Describe the Thermal Performances of a Latent Thermal Storage System during Discharge Period.” *Journal of Energy Storage* 52. doi: 10.1016/j.est.2022.104960.

Saydam, Vahit, Mohammad Parsazadeh, Musaab Radeef, and Xili Duan. 2019. “Design and Experimental Analysis of a Helical Coil Phase Change Heat Exchanger for Thermal Energy Storage.” *Journal of Energy Storage* 21:9–17. doi: 10.1016/j.est.2018.11.006.

Scharinger-Urschitz, Georg, Paul Schwarzmayr, Heimo Walter, and Markus Haider. 2020. “Partial Cycle Operation of Latent Heat Storage with Finned Tubes.” *Applied Energy* 280. doi: 10.1016/j.apenergy.2020.115893.

Tay, N. H. S., M. Belusko, A. Castell, L. F. Cabeza, and F. Bruno. 2014. “An Effectiveness-NTU Technique for Characterising a Finned Tubes PCM System Using a CFD Model.” *Applied Energy* 131:377–85. doi: 10.1016/j.apenergy.2014.06.041.

Yang, Haitian, and Yiqian He. 2010. “Solving Heat Transfer Problems with Phase Change via Smoothed Effective Heat Capacity and Element-Free Galerkin Methods.” *International Communications in Heat and Mass Transfer* 37(4):385–92. doi: 10.1016/j.icheatmasstransfer.2009.12.002.

Yang, Li Wei, Yan Li, Tong Yang, and Hua Sheng Wang. 2022. “Low Temperature Heating Operation Performance of a Domestic Heating System Based on Indirect Expansion Solar Assisted Air Source Heat Pump.” *Solar Energy* 244:134–54. doi: 10.1016/j.solener.2022.08.037.

Yıldız, Çağatay, Mustafa Seçilmiş, Müslüm Arıcı, Mehmet Selçuk Mert, Sandro Nižetić, and Hasan Karabay. 2023. “An Experimental Study on a Solar-Assisted Heat Pump Incorporated with PCM Based Thermal Energy Storage Unit.” *Energy* 278. doi: 10.1016/j.energy.2023.128035.

Zauner, Christoph, Florian Hengstberger, Mark Etzel, Daniel Lager, Rene Hofmann, and Heimo Walter. 2016. “Experimental Characterization and Simulation of a Fin-Tube Latent Heat Storage Using High Density Polyethylene as PCM.” *Applied Energy* 179:237–46. doi: 10.1016/j.apenergy.2016.06.138.

Zhang, X. Y., Y. T. Ge, Burra, and P. Y. Lang. 2024. “Experimental Investigation and CFD Modelling Analysis of Finned-Tube PCM Heat Exchanger for Space Heating.” *Applied Thermal Engineering* 244:122731. doi: 10.1016/j.applthermaleng.2024.122731.

Zhang, Yuting, Zhaoyu He, Weimin Guo, and Peng Zhang. 2024. “Data-Driven Optimization of Packed Bed Thermal Energy Storage Heating System with Encapsulated Phase Change Material.” *Journal of Energy Storage* 79:110017. doi: 10.1016/j.est.2023.110017.

Zsembinszki, Gabriel, Christian Orozco, Jaume Gasia, Tilman Barz, Johann Emhofer, and Luisa F. Cabeza. 2020. “Evaluation of the State of Charge of a Solid/Liquid Phase Change Material in a Thermal Energy Storage Tank.” *Energies* 13(6). doi: 10.3390/en13061425.

https://doi.org/10.52202/077185-0098